

# Sulfenamides as Building Blocks for Efficient Disulfide-Based Self-Healing Materials. A Quantum Chemical Study

Fernando Ruipérez,<sup>\*,[a]</sup> Maialen Galdeano,<sup>[b]</sup> Ekiñe Gimenez,<sup>[b]</sup> and Jon M. Matxain<sup>\*,[b]</sup>

The theoretical self-healing capacity of new sulfenamide-based disulfides is estimated by using theoretical methods of quantum chemistry. Starting from previously studied aromatic disulfides, the influence of inserting a NH group between the disulfide and the phenyl ring (forming the sulfenamide), as well as the role of the phenyl ring in the self-healing process is analyzed. Three parameters are used in the evaluation of the self-healing capacity: i) the probability to generate sulfenyl radicals, which is the first step of the process; ii) the effect of the hydrogen bonding, which affects the mobility of the chains; and iii) the height of the exchange reaction barrier. The insertion of the NH group notably decreases the bond dissociation energy

and, therefore, increases the probability to produce sulfenyl radicals and helps the approach of these radicals to neighboring disulfides, favoring the self-healing process. The role of the phenyl rings is clearly observed in the reaction barriers, where the  $\pi$ - $\pi$  stacking interactions notably stabilize the transition states, resulting in larger rate constants. Nevertheless, this stabilization is somewhat reduced in the aromatic sulfenamides, owing to a less effective  $\pi$ - $\pi$  interaction. Therefore, the sulfenamide-based aromatic disulfides may be considered as promising candidates for the design of efficient self-healing materials.

## 1. Introduction

Smart adaptive materials capable of healing after environmental stress, such as abrasion, impact, oxidation, or moisture, are currently of great interest because of the possibility of improving product functionality and lifetime, reducing the rate of failures, and decreasing the maintenance. The practical demand for maximum usage times leads to the pursuit of self-healing materials.<sup>[1–7]</sup>

Self-healing polymers, in particular, have been explored intensively because of their wide field of application and the large variety of healing mechanisms available.<sup>[8–12]</sup> The healing process is based on reversible chemistry, involving dynamic covalent bonds, non-covalent interactions, or a combination of both. A reversible bond is defined as a chemical linkage that can cleavage and re-form under equilibrium conditions, which may enable polymers to be adaptable by means of structure

modification to favor a more thermodynamically stable state determined by a stimulus.<sup>[13–15]</sup> Thus, the reorganization of the chemical bonds leads to a reconnection of the damaged parts, resulting in a partial or complete recovery of the material. This process may be triggered either by an external stimulus, such as heat,<sup>[16–18]</sup> pressure,<sup>[19]</sup> light,<sup>[20,21]</sup> or automatically (e.g. by the damage itself).<sup>[22]</sup>

To achieve an autonomously healing material, the healing process should take place at ambient conditions and, for that, disulfide bonds appear as good candidates. Disulfide chemistry has been favored in the design of self-healing polymers, owing to the dynamics and reversibility of the S–S bond cleavage.<sup>[23,24]</sup> Nevertheless, most of the synthesized materials are based in aliphatic disulfides, which still need the presence of a catalyst,<sup>[25–29]</sup> irradiation,<sup>[30–33]</sup> or temperature<sup>[34,35]</sup> to undergo the exchange reaction, whereas it would be desirable to have this reaction under mild conditions, without external stimuli. In this sense, aromatic disulfides are found to be especially promising,<sup>[36–38]</sup> and exchange reactions have been reported at room temperature both in solution<sup>[39]</sup> and in the solid state.<sup>[40]</sup> Thus, aromatic disulfides have been used for the preparation of self-healing and reprocessable elastomers,<sup>[41–43]</sup> epoxy networks,<sup>[44–46]</sup> or polyurethanes,<sup>[47]</sup> among others.


The mechanism responsible for the exchange of the disulfide compounds has recently been proposed theoretically by using quantum chemical calculations,<sup>[48]</sup> and confirmed experimentally.<sup>[49]</sup> It consists of a [2+1] radical-mediated mechanism, in which the first step is the homolytic cleavage of the S–S bond to generate sulfenyl radicals that may attack other neighboring disulfide bonds, producing an interchange of sulfur atoms via a three-membered transition state. Several param-


[a] Dr. F. Ruipérez

POLYMAT, University of the Basque Country UPV/EHU  
Joxe Mari Korta Center, Avda. Tolosa 72  
20018 Donostia-San Sebastián (Spain)  
E-mail: fernando.ruiperez@polymat.eu

[b] M. Galdeano, E. Gimenez, Dr. J. M. Matxain

Kimika Fakultatea, Euskal Herriko Unibertsitatea UPV/EHU  
and Donostia International Physics Center (DIPC)  
P.K. 1072, 20080 Donostia, Euskadi (Spain)  
E-mail: jonmattin.matxain@ehu.es

 The ORCID identification number(s) for the author(s) of this article can be found under:  
<https://doi.org/10.1002/open.201800003>.

 © 2018 The Authors. Published by Wiley-VCH Verlag GmbH & Co. KGaA. This is an open access article under the terms of the Creative Commons Attribution Non-Commercial License, which permits use, distribution and reproduction in any medium, provided the original work is properly cited, and is not used for commercial purposes.

ters may affect the evolution of this reaction: a) the concentration of sulfenyl radicals, which can be controlled chemically by tuning the strength of the S–S bond; b) the dynamics of the polymeric chains, governing the ability to flow and reshuffle; and c) the energetic barrier of the exchange process.

The analysis of these three parameters has been performed recently<sup>[48,50]</sup> for a set of aromatic disulfides, leading to a theoretical protocol to estimate the self-healing capacity of a given material. In this manner, it has been observed that electron-donating groups (EDGs) in the phenyl rings, especially the amino group and derivatives, weaken the S–S bond, promoting the formation of sulfenyl radicals. The chain dynamics is analyzed in terms of the non-covalent interactions, in particular the  $\pi$ – $\pi$  stacking and the hydrogen bonding. The former has a slight influence on the mobility of the chains, whereas the latter is relevant in the reaction process: molecular dynamics simulations show that both an excessively large and small number of hydrogen bonds may be detrimental for the process, as estimated by the ratio of disulfides that are close enough to undergo the exchange reaction. Finally, the reaction barrier should be low enough to allow the reaction at room temperature. Barriers of only 12–14 kcal mol<sup>-1</sup> have been calculated for different systems. The influence of the activation energy is accounted for by the exchange reaction constant.

In this work, we intend to estimate the self-healing capacity of several novel urea- and urethane-based disulfide polymers by using the previous theoretical protocol. In particular, two main features will be analyzed: i) the influence of the amino group when it is located between the disulfide and the phenyl group (R–Ph–NH–SS–NH–Ph–R, where R = urea, urethane), that is, the performance of sulfenamide-based aromatic disulfides, and ii) the role of the phenyl rings by studying the same molecular materials without Ph rings (R–SS–R). Although the role of the phenyl group was observed to be marginal in the mobility of the chains,<sup>[50]</sup> it is relevant in the dissociation energy,<sup>[48]</sup> and is expected to play a key role in the stabilization of the three-membered transition state of the exchange reaction, affecting the kinetic barrier. Besides, the photodissociation mechanism of the S–S bond will be discussed. With this mechanism, the sulfenyl radical amount could be increased, thereby helping the self-healing process.

## Computational Methods

All geometry optimizations have been performed in the gas phase by using the long-range corrected wB97XD functional<sup>[51]</sup> within density functional theory (DFT)<sup>[52,53]</sup> in combination with the 6-31+G(d,p) basis set.<sup>[54]</sup> Harmonic vibrational frequencies were obtained at the same level of theory to determine whether the structures were minima or transition states and to evaluate the zero-point vibrational energy (ZPVE) and the thermal ( $T=298$  K) vibrational corrections to the enthalpy ( $H$ ) and Gibbs free energy ( $G$ ) in the harmonic oscillator approximation. Single-point calculations using the 6-311++G(2df,2p) basis set<sup>[55]</sup> were carried out on the optimized structures to refine the electronic energy. To understand the photodissociation process, the same functional was used within the time-dependent density functional theory (TDDFT) framework,<sup>[56]</sup> combined with the 6-31+G(d,p) basis set. All DFT calculations

were carried out by using the Gaussian09 package.<sup>[57]</sup> This methodology was demonstrated to be accurate compared to high-level CASPT2 calculations.<sup>[48]</sup>

In addition, *ab initio* Born-Oppenheimer molecular dynamics (QMD) calculations have been carried out for the optimized species in order to determine their thermal stability, using the PBE functional<sup>[58,59]</sup> combined with a double-zeta quality basis set and the RI formalism, with the corresponding auxiliary basis sets.<sup>[60–62]</sup> This functional has been selected because it was observed to yield similar bond dissociation energies (BDEs) to the  $\omega$ B97XD functional.<sup>[48]</sup> The calculations were carried out at 298 K, by means of the Nose-Hoover thermostat. All these simulations were as long as 40000.00 au (9.651 ps), with a time step of 40.0 au (1.93 ps). These QMD calculations were performed by using the TURBOMOLE package.<sup>[63]</sup>

Finally, the analysis of the population of the natural orbitals have been performed by using the natural bonding orbital (NBO) method.<sup>[64–66]</sup>

## 2. Results

In this work, three molecular models are used for the analysis, based on chemical modification of a diphenyl disulfide *para*-substituted with either urea or urethane moieties (see Figure 1, top), which have been previously studied in our group.<sup>[48,50]</sup> The first modification consists of the insertion of an amino group between the disulfide and the phenyl groups to generate a sulfenamide (Figure 1, middle), and the second involves the removal of the phenyl groups (Figure 1, bottom). Therefore, a total of six systems will be studied.

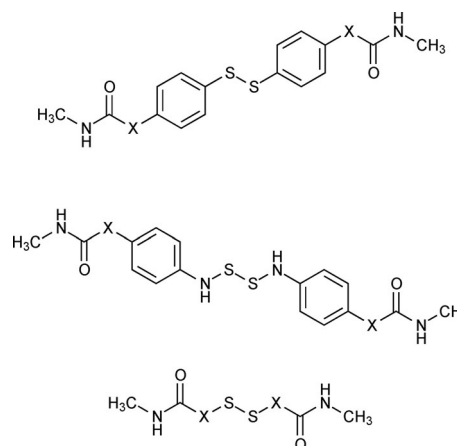


**Figure 1.** Molecular models used in this work. X stands for NH (urea) and O (urethane).

The results are organized as follows: i) the formation of sulfenyl radicals will be discussed using the BDE of the disulfide bond, including the mechanism of the photodissociation process; ii) the influence of the hydrogen bonding in the self-healing process; and iii) the height of the exchange reaction barrier, which will provide an estimation of the rate constant.

## 2.1. Radical Formation

### 2.1.1. Bond Dissociation Energy in Phenyl-Free Disulfides

In this section, preceding the complete analysis of the bond dissociation process in the three models presented above, several phenyl-free disulfides are tested to analyze the effect of the nature of different moieties directly attached to the sulfur atoms on the BDE in order to select those that may weaken the bond, facilitating the radical formation. Thus, the R–SS–R model system is studied in this section, where R stands for both EDGs and electron-withdrawing groups (EWGs).

In Table 1, we have collected the BDEs, the spin densities on the sulfur atom ( $\rho_s$ ), the occupation numbers of the bonding [ $\eta(\sigma_{SS})$ ] and antibonding [ $\eta(\sigma_{SS}^*)$ ] sigma orbitals of the disulfide bond as well as the bond order, defined as [ $\eta(\sigma_{SS}) - \eta(\sigma_{SS}^*)$ ]/2,

R	BDE	$\rho_s$	$\eta(\sigma_{SS})$	$\eta(\sigma_{SS}^*)$	BO( $\sigma_{SS}$ )	$\lambda$	$r_{S-S}^{opt}$
<b>Electron-withdrawing groups (EWGs)</b>							
COOCH <sub>3</sub>	60.70	0.972	1.975	0.018	0.979	245.9	2.05
CN	41.68	0.788	1.955	0.045	0.955	310.5	2.09
CF <sub>3</sub>	64.20	0.976	1.973	0.021	0.976	247.8	2.05
NO <sub>2</sub>	64.35	0.932	1.979	0.034	0.972	280.5	1.97
SO <sub>3</sub> H	68.19	0.930	1.979	0.033	0.973	259.8	2.03
F	75.28	0.935	1.989	0.053	0.968	258.5	1.92
<b>Electron-donating groups (EDGs)</b>							
NH <sub>2</sub>	36.34	0.753	1.984	0.104	0.940	231.7	2.06
OCH <sub>3</sub>	54.91	0.836	1.978	0.099	0.940	232.2	2.01
OH	56.45	0.863	1.985	0.083	0.951	234.0	2.00
CH <sub>3</sub>	58.67	0.968	1.984	0.024	0.980	258.0	2.06
OCOCH <sub>3</sub>	58.19	0.905	1.978	0.049	0.964	261.3	1.98

the excitation energy to the first excited state ( $\lambda$ ), and the optimized sulfur–sulfur bond length ( $r_{S-S}^{opt}$ ). The BDE is calculated as the enthalpy difference in the following process [Eq. (1)]:



It is observed that, in general, the BDE is lower for EDG-containing disulfides, with the lowest value calculated for the diamine disulfide, H<sub>2</sub>N–SS–NH<sub>2</sub> (36.34 kcal mol<sup>-1</sup>). It is worth noting that both the dimethyl (H<sub>3</sub>C–SS–CH<sub>3</sub>) and the diphenyl (Ph–SS–Ph) disulfides show experimental BDEs of 65.2<sup>[67]</sup> and 51.2 kcal mol<sup>-1</sup>,<sup>[68]</sup> respectively (61.0 and 48.0 kcal mol<sup>-1</sup> calculated at the level of theory used in this work<sup>[48]</sup>). The aromatic disulfides were introduced in order to facilitate the self-healing process under mild conditions. In this section, we show that it is possible to design disulfides with weaker S–S bonds without phenyl groups, by including an amino group directly attached to the disulfide. This reduction of the BDE can be ascribed to a greater delocalization of the sulfenyl radical, which is reflected in the low value of the spin density on sulfur (0.753). In ad-

dition, a non-negligible population of the antibonding  $\sigma$  orbital is observed (0.104), reducing the bond order (0.940) and, thus, weakening the S–S bond. As a summary, we can affirm that the amino group is the most suitable to design disulfides with low BDEs, a feature that was previously observed in amino derivatives of aromatic disulfides.<sup>[48]</sup>

The case of the cyanide derivative NC–SS–CN is also remarkable, which, in spite of CN being a strong EWG, shows a BDE of only 41.68 kcal mol<sup>-1</sup>, that is 20–30 kcal mol<sup>-1</sup> lower than other EWG-containing disulfides, and around 15 kcal mol<sup>-1</sup> lower than the EDG derivatives studied in this work, with the exception of diamine disulfide. The cyanide group is also able to efficiently delocalize the sulfenyl radical, as it is observed in the low value of spin density (0.788), and a notable population of the  $\eta(\sigma_{SS}^*)$  antibonding orbital is also observed (0.045). Thus, this group might also be considered as a candidate for weakening the disulfide bond. Nevertheless, in this work, we will only use amino derivatives in the discussion.

### 2.1.2. Thermal Dissociation

In this subsection, we analyze the dissociation of the six model systems represented in Figure 1. In addition to the BDEs, spin densities, population of the orbitals, and optimized S–S bond distances, we have also performed quantum molecular dynamics (QMD) to calculate the maximum and average sulfur–sulfur distances, as well as to estimate the probability to generate sulfenyl radicals ( $\rho$ ), using the following parameter [Eq. (2)]:<sup>[50]</sup>

$$\rho = \frac{N_{S-S}}{N_{tot}} \quad (2)$$

where  $N_{S-S}$  is the number of simulation steps with S–S bonds larger than a threshold value of 2.3 Å and  $N_{tot}$  is the total number of simulation steps. This threshold is estimated from quantum chemical calculations, in which the minimum S–S distance for the transition states to generate the sulfenyl radicals were slightly larger than 2.3 Å.<sup>[48]</sup>

The first two rows in Table 2 correspond to the aromatic disulfides with urea (NH–CO–NH–CH<sub>3</sub>) and urethane (O–CO–NH–CH<sub>3</sub>) groups in the *para* position of the phenyl rings. These systems have been previously studied,<sup>[48,50]</sup> and will serve as a reference for the discussion along the manuscript. We observe that the urea derivative, which is a *para*-amino-phenyl derivative, shows a slightly lower BDE and spin density than the urethane derivative, owing to a greater delocalization of the sulfenyl radical. As a consequence, the urea derivative presents a larger probability to generate radicals ( $\rho = 0.005$ ) than the urethane ( $\rho = 0.001$ ).

Inspecting the results for the sulfenamides, that is, with an amino group inserted between the disulfide and the phenyl ring (rows 3 and 4 in Table 2), we observe a remarkable decrease in the BDE in both cases, of around 15 kcal mol<sup>-1</sup>, which is the consequence of the combination of a very low spin density on sulfur (around 0.67) and a large population of the antibonding  $\sigma_{SS}^*$  orbital (around 0.15). Therefore, the bond order is far from being a regular single bond (0.91). As the results for

**Table 2.** BDEs [ $\text{kcal mol}^{-1}$ ],  $\rho_S$ ,  $\eta$  for the bonding and antibonding  $\sigma_{SS}$  orbitals, BO of the disulfide bond, and optimized sulfur-sulfur bond length ( $r_{S-S}^{\text{opt}}$ ) [ $\text{\AA}$ ], calculated at the  $\omega\text{B97XD}/6\text{-}311++\text{G}(2\text{df},2\text{p})/\omega\text{B97XD}/6\text{-}31+\text{G}(\text{d},\text{p})$  level of theory.  $r_{S-S}^{\text{max}}$  and  $r_{S-S}^{\text{ave}}$  correspond to the maximum and average sulfur-sulfur bond distances [ $\text{\AA}$ ] and  $\rho$  is the probability to generate sulfenyl radicals, calculated by means of QMD simulations.

	DFT BDE	$\rho_S$	$\eta(\sigma_{SS})$	$\eta(\sigma_{SS}^*)$	BO( $\sigma_{SS}$ )	$r_{S-S}^{\text{opt}}$	QMD $r_{S-S}^{\text{max}}$	$r_{S-S}^{\text{ave}}$	$\rho$
SS-Ph-NH-CO-NH-CH <sub>3</sub>	48.55	0.769	1.960	0.058	0.951	2.11	2.31	2.12	0.005
SS-Ph-O-CO-NH-CH <sub>3</sub>	51.99	0.804	1.961	0.052	0.955	2.11	2.33	2.12	0.001
SS-NH-Ph-NH-CO-NH-CH <sub>3</sub>	34.08	0.667	1.976	0.149	0.913	2.10	2.50	2.21	0.234
SS-NH-Ph-O-CO-NH-CH <sub>3</sub>	36.08	0.679	1.976	0.145	0.916	2.10	2.38	2.19	0.089
SS-NH-CO-NH-CH <sub>3</sub>	47.65	0.804	1.977	0.117	0.930	2.08	2.33	2.15	0.068
SS-O-CO-NH-CH <sub>3</sub>	55.56	0.868	1.978	0.079	0.949	2.01	2.12	2.00	0.000

the urea and urethane derivatives are basically the same, this feature may be ascribed to the presence of the NH group adjacent to the disulfide, which is consistent with the results discussed in the previous subsection. Regarding the optimized S-S bond distance ( $r_{S-S}^{\text{opt}}$ ), it remains almost unaltered (2.10–2.11  $\text{\AA}$ ); however, both the average and maximum sulfur-sulfur distances obtained from the QMD simulations are notably larger, which means that the bond is actually weaker and easier to be thermally cleaved. This is clearly manifested in the probability to generate sulfenyl radicals, which is much larger in these systems, especially for the urea derivative (0.234). Thus, the presence of an amino group between the disulfide and the phenyl ring has a dramatic effect in the generation of radicals.

Finally, the last two rows in Table 2 correspond to the diurea and diurethane disulfides, where the aromatic rings have been removed. In these cases, it is observed that the BDE remains essentially unchanged for the urea derivative with respect to the aromatic counterpart, and is slightly increased in the urethane case. This effect is strongly manifested in the QMD simulations, where somewhat longer values of both the maximum and average S-S distances are obtained for the urea, whereas those of the urethane are notably shorter. As a result, the probability to generate sulfenyl radicals is increased one order of magnitude (0.068 vs. 0.005) in the case of the urea, whereas for the urethane this probability is negligible. This result may be related to the rather large population in the antibonding  $\sigma_{SS}^*$  orbital in the urea derivative (0.117) compared to that of the aromatic disulfide (0.058) and, as a consequence, a lower bond order (0.930 vs. 0.951) and higher probability to create sulfenyl radicals. Therefore, we can conclude that removing the phenyl ring is advantageous in order to generate radicals in the urea derivative, probably owing to the nature of the sulfenamide bond.

### 2.1.3. Photodissociation

To analyze the photodissociation of the disulfide bond, we have calculated the first three lowest vertical transitions for each model system. The absorption wavelengths ( $\lambda_i$ ) and their corresponding oscillator strengths ( $f_i$ ) have been calculated, and their values are given in Table 3, along with the nature of

**Table 3.** Absorption wavelengths ( $\lambda_i$ ) [nm] of the lowest three excited states, oscillator strength ( $f_i$ ) and the lowest unoccupied molecular orbitals (LUMO) involved in the transition.

X	$\lambda_1$	$f_1$	LUMO	$\lambda_2$	$f_2$	LUMO	$\lambda_3$	$f_3$	LUMO
<b>SS-Ph-X-CO-NH-CH<sub>3</sub></b>									
NH	359.9	0.010	$\sigma_{SS}^*$	265.6	0.199	$\sigma_{SS}^*$	256.1	0.047	$\sigma_{SS}^*$
O	357.1	0.007	$\sigma_{SS}^*$	251.6	0.031	$\sigma_{SS}^*$	247.1	0.005	$\sigma_{SS}^*$
<b>SS-NH-Ph-X-CO-NH-CH<sub>3</sub></b>									
NH	292.5	0.151	$\sigma_{SS}^*$	263.9	0.029	$\sigma_{SS}^*$	258.5	0.115	$\sigma_{SS}^*$
O	282.9	0.173	$\sigma_{SS}^*$	256.0	0.084	$\sigma_{SS}^*$	251.5	0.033	$\sigma_{SS}^*$
<b>SS-X-CO-NH-CH<sub>3</sub></b>									
NH	239.0	0.034	$\sigma_{SS}^*$	221.6	0.015	$\sigma_{SS}^*$	217.8	0.224	$\sigma_{SS}^*$
O	232.1	0.000	$\sigma_{SS}^*$	229.3	0.000	$\sigma_{SS}^*$	222.0	0.015	$\sigma_{SS}^*$

the lowest unoccupied molecular orbital (LUMO), which is the populated orbital after the excitation in all the studied cases. These LUMO orbitals are depicted in Figure 2.

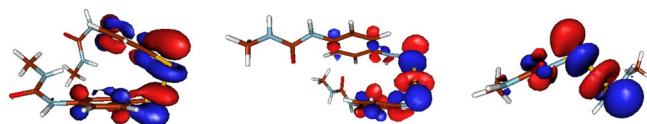


**Figure 2.** LUMO of the urea-based derivatives for the aromatic disulfides (left), the sulfenamides with the amino group inserted between the SS and the Ph ring (center), and phenyl-free derivatives (right).

Looking at the data collected in Table 3, it can be observed that all transitions correspond to excitations in the UV region and, hence, the photodissociation will not contribute to the generation of radicals under ambient conditions. The presence of phenyl rings induces a redshift in the transitions, owing to the participation of the  $\pi$  molecular orbitals, which are located at higher energies than the  $\sigma$  molecular orbital of the S-S bond. The oscillator strengths are found to be non-zero for all calculated excitations (except for the urethane-based phenyl-free disulfide). Clearly, the intensity of the transitions with larger oscillator strengths will also be larger but, from a qualitative point of view, we observe that the behavior is similar in all cases. It is also observed that, regardless of the absorption

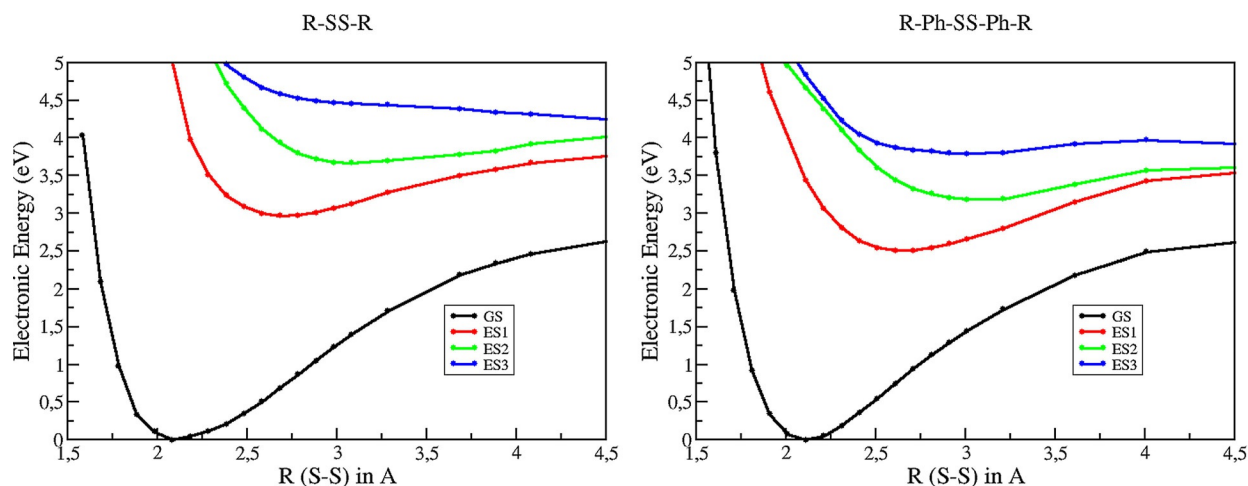


**Figure 3.** Potential energy surfaces for the ground and first three lowest excited states as function of the S–S bond distance for the SS–NH–CO–NH–CH<sub>3</sub> (left) and SS–Ph–NH–CO–NH–CH<sub>3</sub> (right) derivatives.

wavelength and oscillator strength, the electron is excited to the  $\sigma_{SS}^*$  antibonding molecular orbital. Hence, all of these excitations should considerably decrease the BDE of the S–S bond in the excited states. To check for this, we calculated the evolution of the excited states once the transitions take place.

To check if this excitation process would lead to dissociation of the S–S bond, we calculated the potential energy surfaces (PES) for the three lowest excited states. In Figure 3, the calculated PES values are depicted as a function of the S–S distance. For simplicity, only the R–SS–R and R–Ph–SS–Ph–R cases are represented. In all cases, the equilibrium S–S bond is significantly elongated and, hence, once the absorption takes place, the BDE is considerably reduced and dissociation may take place. As the process needs UV light, this way of producing sulfenyl radicals will not take place in these materials unless they are externally irradiated and, therefore, at ambient conditions and without irradiation, the radicals may only be generated with thermal activation.

## 2.2. Hydrogen Bonding

Non-covalent interactions play a relevant role in polymeric materials. For instance, the presence of hydrogen bonds in the repeating unit of the polymer affects the crystallization of the material, stabilizing adjacent chains. In our previous work,<sup>[50]</sup> we observed that the hydrogen bonding is a key structural characteristic in disulfide-based self-healing materials, influencing the flexibility and mobility of the polymeric chains. In this sense, by means of classical molecular dynamics, we estimated the mobility in terms of the number of hydrogen bonds established among chains and calculated the ratio of disulfides ( $\omega$ ) that were located within a spatial region, close enough to undergo the exchange reaction. Thus, the larger the number of disulfides in this region ( $\omega$ ), the larger the probability to react.

In this work, as we are only using small model systems and quantum mechanical methods, it is not possible to accurately estimate the  $\omega$  parameter. Instead, we calculate the interaction energy between two disulfide molecules caused by the pres-

ence of hydrogen bonds, which will allow us to perform a reasonable estimate of the magnitude of  $\omega$  in terms of the  $r_{S-S}^{opt}$  values, that is, from the distances between the disulfides obtained both in the DFT and in the QMD calculations, which are collected in Table 4.

Two conformations have been explored, denoted as conformation 1 and 2, depending on the relative disposition of the disulfides. Comparing the results for urea- and urethane-based aromatic disulfides (first two rows in Table 4), similar interaction energies and sulfur–sulfur distances are calculated, although somewhat shorter distances are observed in the urea derivative. When the NH group is inserted between the aromatic ring and the SS moiety to generate the sulfenamide, a general decrease of the  $r_{S-S}^{opt}$  distances is found (see rows 3 and 4), which may imply larger values of the previously mentioned  $\omega$  parameter, as there is a larger probability for the disulfides to get closer. Regarding the interaction energies, a clear increase is observed in the urea derivative, as the NH group is more efficient in establishing hydrogen bonding interactions. For the urethane derivative, the variation is smaller and a slight decrease is observed. Finally, when the phenyl group is removed (last two rows), dramatic changes are observed: although the interaction energies are smaller for the urea-based derivative and not for the urethane, the contraction observed in the sulfur distances for the two molecular systems is remarkable, that is, between 3 and 4 Å. This means that the disulfides are allowed to get closer and, therefore, may imply notably larger values of  $\omega$  than in the aromatic disulfides.

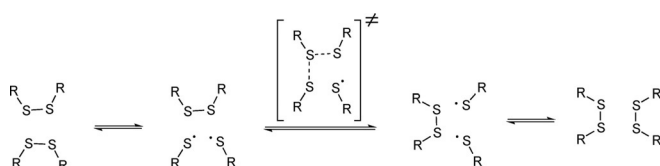
## 2.3. Reaction Mechanism

As stated in the Introduction, the prevalent mechanism of the self-healing process in disulfide-based materials is a [2+1] radical-mediated mechanism,<sup>[48,49]</sup> in which the generated sulfenyl radicals attack other disulfides found in the vicinity via a three-membered transition state, as represented in Figure 4.

This section is devoted to the analysis of this transition state, that is, the kinetic barrier, which is a key feature for the

**Table 4.** Interaction energy caused by the presence of hydrogen bonds in conformations 1 ( $\Delta H_1^{\text{HB}}$ ) and 2 ( $\Delta H_2^{\text{HB}}$ ) [ $\text{kcal mol}^{-1}$ ].  $r_{\text{S-S}}^{\text{opt}}$  stands for the minimum and maximum S–S distance among the four S atoms in each configuration [ $\text{\AA}$ ], whereas  $r_{\text{S-S}}^{\text{min}}$  and  $r_{\text{S-S}}^{\text{max}}$  are the same distances calculated in the QMD simulations.

	DFT $\Delta H_1^{\text{HB}}$	$r_{\text{S-S}}^{\text{opt}}$	$\Delta H_2^{\text{HB}}$	$r_{\text{S-S}}^{\text{opt}}$	QMD $r_{\text{S-S}}^{\text{min}}$	$r_{\text{S-S}}^{\text{max}}$
SS–Ph–NH–CO–NH–CH <sub>3</sub>	30.40	7.72–9.93	25.41	12.33–13.01	6.42	13.82
SS–Ph–O–CO–NH–CH <sub>3</sub>	33.64	9.22–9.87	26.45	11.56–12.67	8.38	14.08
SS–NH–Ph–NH–CO–NH–CH <sub>3</sub>	38.45	5.14–8.62	40.84	11.10–13.20	7.10	14.42
SS–NH–Ph–O–CO–NH–CH <sub>3</sub>	26.16	7.33–9.58	26.94	12.72–14.57	7.44	13.80
SS–NH–CO–NH–CH <sub>3</sub>	22.33	4.16–5.87	19.18	4.68–6.36	3.34	6.94
SS–O–CO–NH–CH <sub>3</sub>	32.24	5.06–5.80	32.69	6.31–6.59	3.48	8.04

**Figure 4.** Representation of the [2+1] radical-mediated exchange reaction mechanism.

self-healing process to occur at room temperature or at relatively low temperatures. Thus, the geometric parameters of the reactant complex and transition state, as well as the Gibbs free energy of the latter, are collected in Table 5. The exchange reaction constant is estimated by using the transition state theory of Wigner, Eyring, Polanyi, and Evans [Eq. (3)]:<sup>[69,70]</sup>

$$k = \frac{k_B T}{h} e^{-\Delta G^{\ddagger}/RT} \quad (3)$$

Inspecting the geometries of the reactant complex, it is observed that the radical is located between 4.42 and 8.16  $\text{\AA}$ . In aromatic derivatives, this distance is, in general, smaller (4.42–4.58  $\text{\AA}$ ) than in the NH–Ph derivatives (4.49–5.15  $\text{\AA}$ ). In the phenyl-free systems, the radical is located at greater distances, between 6.17–8.16  $\text{\AA}$ . Considering the transition state, the average distance among the three sulfur atoms is 2.43  $\text{\AA}$  in the aromatic disulfides, 2.53  $\text{\AA}$  in the derivatives with the NH group inserted, and only 2.34  $\text{\AA}$  for the phenyl-free disulfides

without. This distance is particularly low in the urethane derivative, around 2.26  $\text{\AA}$ . Finally, the most important parameter is the barrier height, measured as the Gibbs free energy of the transition state ( $\Delta G^{\ddagger}$ ). It is clearly observed that this barrier is lower in the aromatic disulfides (11–12  $\text{kcal mol}^{-1}$ ), which is increased to 16–18  $\text{kcal mol}^{-1}$  when the NH is located between the phenyl and the disulfide, and even a bit higher when the Ph group is absent. This gives us an idea of the role of the phenyl ring, which may stabilize the transition state through  $\pi$ – $\pi$  stacking. This interaction is notably quenched when the amino group is located adjacent to the SS, changing the relative disposition of the phenyl rings and separating them. This is clearly reflected in the calculated rate constants, which are several orders of magnitude larger for the aromatic disulfides.

### 3. Conclusions

In this work, we performed a detailed theoretical analysis of new urea- and urethane-based disulfides for their use as self-healing materials. In particular, starting from previously studied aromatic disulfides, we have investigated i) the influence of inserting an amino group between the disulfide bond and the phenyl ring, generating sulfenamide-based aromatic disulfides, and ii) the role of the Ph rings in the self-healing process. We have estimated the theoretical self-healing capacity of these new derivatives making use of three features, namely, the S–S bond dissociation energy (both thermal and photodissociation)

**Table 5.** Geometric and energetic parameters of the reactant complex and the transition state. Sulfur–sulfur distances ( $r_{\text{S}_1-\text{S}_2}$  and  $r_{\text{S}_2-\text{S}_3}$ ) [ $\text{\AA}$ ], ( $\text{S}_1, \text{S}_2, \text{S}_3$ ) angles ( $\alpha$ ) [ $^\circ$ ], Gibbs free energies ( $\Delta G^{\ddagger}$ ) [ $\text{kcal mol}^{-1}$ ], and rate constants ( $k$ ) [ $\text{s}^{-1}$ ].

	Reactant complex			Transition state			$\Delta G^{\ddagger}$	$k$
	$r_{\text{S}_1-\text{S}_2}$	$r_{\text{S}_2-\text{S}_3}$	$\alpha$	$r_{\text{S}_1-\text{S}_2}$	$r_{\text{S}_2-\text{S}_3}$	$\alpha$		
SS–Ph–NH–CO–NH–CH <sub>3</sub>	2.14	4.58	147.9	2.44	2.44	156.4	11.04	$4.973 \times 10^4$
SS–Ph–O–CO–NH–CH <sub>3</sub>	2.14	4.42	152.9	2.40	2.42	151.9	12.22	$6.780 \times 10^3$
SS–NH–Ph–NH–CO–NH–CH <sub>3</sub>	2.14	4.49	137.9	2.51	2.56	164.9	18.27	$2.456 \times 10^{-1}$
SS–NH–Ph–O–CO–NH–CH <sub>3</sub>	2.12	5.15	142.3	2.50	2.53	161.1	16.02	$1.107 \times 10^1$
SS–NH–CO–NH–CH <sub>3</sub>	2.08	6.17	110.4	2.39	2.42	165.6	18.51	$1.663 \times 10^{-1}$
SS–O–CO–NH–CH <sub>3</sub>	2.00	8.16	98.0	2.25	2.28	156.5	17.48	$9.415 \times 10^{-1}$

and the probability to form sulfenyl radicals, the effect of hydrogen bonding, and the exchange reaction barrier.

Regarding the dissociation of the disulfide, we have observed that inserting an amino group between the disulfide and the phenyl ring dramatically decreases the BDE and, therefore, notably increases the probability of generating sulfenyl radicals, the first step of the reaction. The BDEs of the phenyl-free derivatives are very similar to those of the aromatic disulfides; nevertheless, the probability of forming sulfenyl radicals in the urea derivative (non-aromatic sulfenamide) is particularly large compared to that for the aromatic counterpart. The photodissociation process needs UV light to take place in all cases. Thus, at room temperature, the most efficient materials to generate radicals are the aromatic sulfenamides. Considering the hydrogen bonding, it is difficult to devise a trend in the interaction energies; however, it is clear that by disconnecting the SS and the Ph moieties, either by inserting a NH group or by removing the phenyl ring, the disulfides are allowed to get closer, thereby increasing the probability to undergo the exchange reaction. A better estimation of the effect of the hydrogen bonding would demand the use of larger models and classical molecular dynamics, which is out of the scope of this work. Finally, inspecting the exchange reaction barriers, it is clear the presence of the phenyl rings adjacent to the S–S bond stabilizes the transition state, probably due to  $\pi$ – $\pi$  stacking interactions, and much larger rate constants are calculated.

Thus, the insertion of a NH group to generate a sulfenamide favors the first step of the self-healing mechanism, increasing the concentration of radicals. In addition, the distances between disulfides are smaller, helping the approach of the radicals to neighboring disulfides and facilitating the conditions for the reaction to occur. Nevertheless, larger barriers (lower rate constants) are accomplished, probably owing to the reduction of the  $\pi$ – $\pi$  interactions among the phenyl rings, which stabilize the transition states. As a conclusion, the sulfenamide-based aromatic disulfides (R–Ph–NH–SS–NH–Ph–R) seem to be promising candidates for new, improved self-healing materials.

## Acknowledgements

Technical and human support provided by IZO-SGI, SGIker (UPV/EHU, MICINN, GV/EJ, ERDF and ESF) is gratefully acknowledged for assistance and generous allocation of computational resources. Financial support comes from Eusko Jaurlaritz through projects IT588-13 and PI2017-11.

## Conflict of Interest

The authors declare no conflict of interest.

**Keywords:** computational chemistry · density functional calculations · disulfenamides · photodissociation · self-healing

[1] Y. Yang, M. W. Urban, *Chem. Soc. Rev.* **2013**, *42*, 7446.

- [2] "An Introduction to Material Design Principles: Damage prevention versus Damage Management": S. van der Zwaag, *Springer Series in Materials Science, Vol. 100*, Springer, Dordrecht, **2007**, pp. 1–18.
- [3] S. J. Rowan, J. P. Capadona, K. Shanmuganathan, D. J. Tyler, C. Weder, *Science* **2008**, *319*, 1370.
- [4] R. Abbel, C. Grenier, M. J. Pouderoijen, J. W. Stouwdam, P. E. L. G. Leclère, R. P. Sijbesma, E. W. Meijer, A. P. H. J. Schenning, *J. Am. Chem. Soc.* **2009**, *131*, 833.
- [5] N. K. Guimard, K. K. Oehlenschlaeger, J. Zhou, S. Hilf, F. G. Schmidt, C. Barner-Kowollik, *Macromol. Chem. Phys.* **2012**, *213*, 131.
- [6] "Principles of Self-Healing Polymers": D. Döhler, P. Michael, W. Binder, *Self-Healing Polymers: From Principles to Applications*, Wiley-VCH, Weinheim, **2013**, pp. 1–60.
- [7] X. K. D. Hillewaere, F. E. Du Prez, *Prog. Polym. Sci.* **2015**, *49*, 121.
- [8] M. D. Hager, P. Greil, C. Leyens, S. van der Zwaag, U. S. Schubert, *Adv. Mater.* **2010**, *22*, 5424.
- [9] M. Q. Zhang, M. Z. Rong, *Polym. Chem.* **2013**, *4*, 4878.
- [10] S. Billiet, X. K. D. Hillewaere, R. F. A. Teixeira, F. E. Du Prez, *Macromol. Rapid Commun.* **2013**, *34*, 290.
- [11] D. Y. Wu, S. Meure, D. Solomon, *Prog. Polym. Sci.* **2008**, *33*, 479.
- [12] N. Kuhl, S. Bode, M. D. Hager, U. S. Schubert, *Adv. Polym. Sci.* **2016**, *273*, 1.
- [13] S. J. Rowan, S. J. Cantrill, G. R. L. Cousins, J. K. M. Sanders, J. F. Stoddart, *Angew. Chem. Int. Ed.* **2002**, *41*, 898; *Angew. Chem.* **2002**, *114*, 938.
- [14] W. Zou, J. Dong, Y. Luo, Q. Zhao, T. Xie, *Adv. Mater.* **2017**, *29*, 1606100.
- [15] N. Roy, B. Bruchmann, J.-M. Lehn, *Chem. Soc. Rev.* **2015**, *44*, 3786.
- [16] S. Burattini, B. W. Greenland, D. Hermida-Merino, W. Weng, J. Seppala, H. M. Colquhoun, W. Hayes, M. E. Mackay, I. W. Hamley, S. J. Rowan, *J. Am. Chem. Soc.* **2010**, *132*, 12051.
- [17] R. Nicolaÿ, J. Kamada, A. Van Wassen, K. Matyjaszewski, *Macromolecules* **2010**, *43*, 4355.
- [18] X. Chen, M. A. Dam, K. Ono, A. Mal, H. Shen, S. R. Nutt, K. Sheran, F. Wudl, *Science* **2002**, *295*, 1698.
- [19] P. Cordier, F. Tournilhac, C. Soulié-Ziakovic, L. Leibler, *Nature* **2008**, *451*, 977.
- [20] Y. Amamoto, J. Kamada, H. Otsuka, A. Takahara, K. Matyjaszewski, *Angew. Chem. Int. Ed.* **2011**, *50*, 1660; *Angew. Chem.* **2011**, *123*, 1698.
- [21] B. T. Michal, C. A. Jaye, E. J. Spencer, S. J. Rowan, *ACS Macro Lett.* **2013**, *2*, 694.
- [22] S. R. White, N. R. Sottos, P. H. Geubelle, J. S. Moore, M. R. Kessler, S. R. Srimam, E. N. Brown, S. Viswanathan, *Nature* **2001**, *409*, 794.
- [23] J. Canadell, H. Goossens, B. Klumperman, *Macromolecules* **2011**, *44*, 2536.
- [24] A. Takahashi, T. Ohishi, R. Goseki, H. Otsuka, *Polymer* **2016**, *82*, 319.
- [25] R. Caraballo, M. Rahm, P. Vongvilai, T. Brinck, O. Ramstrom, *Chem. Commun.* **2008**, 6603.
- [26] J. A. Yoon, J. Kamada, K. Koynov, J. Mohin, R. Nicolaÿ, Y. Zhang, A. C. Balazs, T. Kowalewski, K. Matyjaszewski, *Macromolecules* **2012**, *45*, 142.
- [27] N. V. Tsarevsky, K. Matyjaszewski, *Macromolecules* **2002**, *35*, 9009.
- [28] J. K. Oh, C. B. Tang, H. F. Gao, N. V. Tsarevsky, K. Matyjaszewski, *J. Am. Chem. Soc.* **2006**, *128*, 5578.
- [29] Z. Q. Lei, H. P. Xiang, Y. J. Yuan, M. Z. Rong, M. Q. Zhang, *Chem. Mater.* **2014**, *26*, 2038.
- [30] W. M. Xu, M. Z. Rong, M. Q. Zhang, *J. Mater. Chem. A* **2016**, *4*, 10683.
- [31] Y. Amamoto, H. Otsuka, A. Takahara, K. Matyjaszewski, *Adv. Mater.* **2012**, *24*, 3975.
- [32] H. Otsuka, S. Nagano, Y. Kobashi, T. Maeda, A. Takahara, *Chem. Commun.* **2010**, *46*, 1150.
- [33] B. D. Fairbanks, S. P. Singh, C. N. Bowman, K. S. Anseth, *Macromolecules* **2011**, *44*, 2444.
- [34] U. Lafont, H. van Zeijl, S. van der Zwaag, *ACS Appl. Mater. Interfaces* **2012**, *4*, 6280.
- [35] L. Imberson, E. K. Oikonomou, S. Norvez, L. Leibler, *Polym. Chem.* **2015**, *6*, 4271.
- [36] T. Ohishi, Y. Iki, K. Imato, Y. Higaki, A. Takahara, H. Otsuka, *Chem. Lett.* **2013**, *42*, 1346.
- [37] R. Martin, A. Rekondo, A. Ruiz de Luzuriaga, P. Casuso, D. Dupin, G. Cabañero, H.-J. Grande, I. Odriozola, *Smart Mater. Struct.* **2016**, *25*, 084017.
- [38] I. Azcune, I. Odriozola, *Eur. Polym. J.* **2016**, *84*, 147.
- [39] R. J. Sarma, S. Otto, J. R. Nitschke, *Chem. Eur. J.* **2007**, *13*, 9542.

- [40] A. M. Belenguer, T. Frišćić, G. M. Day, J. K. M. Sanders, *Chem. Sci.* **2011**, *2*, 696.
- [41] R. Martin, A. Rekondo, A. Ruiz de Luzuriaga, G. C. nero, H.-J. Grande, I. Odriozola, *J. Mater. Chem. A* **2014**, *2*, 5710.
- [42] A. Rekondo, R. Martin, A. Ruiz de Luzuriaga, G. Cabañero, H. J. Grande, I. Odriozola, *Mater. Horiz.* **2014**, *1*, 237.
- [43] R. Martin, A. Rekondo, A. Ruiz de Luzuriaga, A. Santamaria, I. Odriozola, *RSC Adv.* **2015**, *5*, 17514.
- [44] A. Ruiz de Luzuriaga, R. Martin, N. Markaide, A. Rekondo, G. Cabañero, J. Rodríguez, I. Odriozola, *Mater. Horiz.* **2016**, *3*, 241.
- [45] L. M. Johnson, E. Ledet, N. D. Huffman, S. L. Swarner, S. D. Shepherd, P. G. Durham, G. D. Rothrock, *Polymer* **2015**, *64*, 84.
- [46] A. Ruiz de Luzuriaga, J. M. Matxain, F. Ruipérez, R. Martin, J. M. Asua, G. Cabañero, I. Odriozola, *J. Mater. Chem. C* **2016**, *4*, 6220.
- [47] R. H. Aguirresarobe, L. Martin, M. J. Fernández-Berridi, L. Irusta, *Express Polym. Lett.* **2017**, *11*, 266.
- [48] J. M. Matxain, J. M. Asua, F. Ruipérez, *Phys. Chem. Chem. Phys.* **2016**, *18*, 1758.
- [49] S. Nevejans, N. Ballard, J. I. Miranda, B. Reck, J. M. Asua, *Phys. Chem. Chem. Phys.* **2016**, *18*, 27577.
- [50] E. Formoso, J. M. Asua, J. M. Matxain, F. Ruipérez, *Phys. Chem. Chem. Phys.* **2017**, *19*, 18461.
- [51] J.-D. Chai, M. Head-Gordon, *Phys. Chem. Chem. Phys.* **2008**, *10*, 6615.
- [52] P. Hohenberg, W. Kohn, *Phys. Rev. B* **1964**, *136*, B864.
- [53] W. Kohn, L. J. Sham, *Phys. Rev.* **1965**, *140*, A1133.
- [54] W. J. Hehre, R. Ditchfield, J. A. Pople, *J. Chem. Phys.* **1972**, *56*, 2257.
- [55] R. Krishnan, J. S. Binkley, R. Seeger, J. A. Pople, *J. Chem. Phys.* **1980**, *72*, 650.
- [56] E. Runge, E. K. U. Gross, *Phys. Rev. Lett.* **1984**, *52*, 997.
- [57] M. J. Frisch, G. W. Trucks, H. B. Schlegel, G. E. Scuseria, M. A. Robb, J. R. Cheeseman, G. Scalmani, V. Barone, B. Mennucci, G. A. Petersson, H. Nakatsuji, M. Caricato, X. Li, H. P. Hratchian, A. F. Izmaylov, J. Bloino, G. Zheng, J. L. Sonnenberg, M. Hada, M. Ehara, K. Toyota, R. Fukuda, J. Hasegawa, M. Ishida, T. Nakajima, Y. Honda, O. Kitao, H. Nakai, T. Vreven, J. A. Montgomery, Jr., J. E. Peralta, F. Ogliaro, M. Bearpark, J. J. Heyd, E. Brothers, K. N. Kudin, V. N. Staroverov, R. Kobayashi, J. Normand, K. Raghavachari, A. Rendell, J. C. Burant, S. S. Iyengar, J. Tomasi, M. Cossi, N. Rega, J. M. Millam, M. Klene, J. E. Knox, J. B. Cross, V. Bakken, C. Adamo, J. Jaramillo, R. Gomperts, R. E. Stratmann, O. Yazyev, A. J. Austin, R. Cammi, C. Pomelli, J. W. Ochterski, R. L. Martin, K. Morokuma, V. G. Zakrzewski, G. A. Voth, P. Salvador, J. J. Dannenberg, S. Dapprich, A. D. Daniels, Ö. Farkas, J. B. Foresman, J. V. Ortiz, J. Cioslowski, D. J. Fox, *Gaussian 09 Revision D.01*, gaussian Inc. Wallingford CT 2009.
- [58] J. P. Perdew, K. Burke, H. Ernzerhof, *Phys. Rev. Lett.* **1996**, *77*, 3865.
- [59] J. P. Perdew, K. Burke, H. Ernzerhof, *Phys. Rev. Lett.* **1997**, *78*, 1396.
- [60] P. Deglmann, K. May, F. Furche, R. Ahlrichs, *Chem. Phys. Lett.* **2004**, *384*, 103.
- [61] O. T. K. Eichkorn, H. Öhm, M. Häser, R. Ahlrichs, *Chem. Phys. Lett.* **1995**, *240*, 283.
- [62] A. Sierka, A. Hogekamp, R. Ahlrichs, *J. Chem. Phys.* **2003**, *118*, 9136.
- [63] TURBOMOLE version 6.6 a development of University of Karlsruhe and Forschungszentrum Karlsruhe GmbH, 1989–2007, TURBOMOLE GmbH, since 2007; available from <http://www.turbomole.com>.
- [64] A. E. Reed, R. B. Weinstock, F. Weinhold, *J. Chem. Phys.* **1985**, *83*, 735.
- [65] A. E. Reed, F. Weinhold, *J. Chem. Phys.* **1985**, *83*, 1736.
- [66] A. E. Reed, L. A. Curtiss, F. Weinhold, *Chem. Rev.* **1988**, *88*, 899.
- [67] J. M. Nicovich, K. D. Kreutter, C. A. van Dijk, P. H. Wine, *J. Phys. Chem.* **1992**, *96*, 2518.
- [68] *Thermochemical Data of Organic Compounds* (Eds.: J. B. Pedley, R. D. Naylor, S. Kirby), Chapman and Hall, New York, **1986**.
- [69] M. G. Evans, M. Polanyi, *Trans. Faraday Soc.* **1935**, *31*, 875.
- [70] H. Eyring, *J. Chem. Phys.* **1935**, *3*, 107.

---

Received: January 3, 2018